

A Comparison between Pulse Width Modulation Strategies in terms of Power Losses in a Three-Phased Inverter - Application to a Starter Generator

J. Hobraiche¹, J.P. Vilain², M. Chemin³

^{1,2} University of Technology of Compiègne
Laboratory of Electromechanics / BP20529
60205 Compiègne Cedex / France

³ Valeo Electrical System
2, rue A. Boulle / BP 150
94017 Créteil Cedex / France

¹Phone +33(0) 344234507 Fax: +33(0) 344237937 E-Mail: Julien.Hobraiche@hds.utc.fr WWW: http://www.utc.fr/lec

²Phone +33(0) 344234507 Fax: +33(0) 34237937 E-Mail: Jean-Paul.Vilain@utc.fr WWW: http://www.utc.fr/lec

³Phone +33(0) 148988442 Fax: +33(0) 142071514 E-Mail: Michael.Chemin@valeo.com WWW: http://www.valeo.com

Abstract – A comparison between Space Vector Modulation and Generalized Discontinuous PWM in terms of power losses in an inverter is presented. Power losses are calculated from PSPICE™ simulation results and data sheets. Each strategy is evaluated by the power losses in the inverter and torque ripple of the starter generator as a function of torque and speed.

I. INTRODUCTION

The opportunities offered by a starter-generator (SG) are multiple. It first allows merging two electrical machines into one to reduce price. New functions can be added such as “Stop and Go”, “Boost”, etc. It also constitutes one possibility to reduce carbon dioxide emission (Kyoto Accord) by substituting diesel propulsion with electrical propulsion whenever thermal engine is polluting [1].

However, SG application implies high constraints because the electrical machine needs a wide range of operating points [2]. In starter mode it requires high torque at low speed and, in alternator mode, electrical power at medium and high speeds.

Here, a synchronous wound rotor machine supplied by a battery through a three-phased inverter is considered [3]. The inverter is heavily solicited because of high currents (up to 800 A) and high switching frequency (20 kHz). We propose to compare Pulse Width Modulation (PWM) strategy in terms of power losses in the inverter and torque ripple in the SG.

Firstly, power losses in the inverter are interpolated from PSPICE™ simulations and MOSFET data sheets [4]. Secondly, power losses in the converter and torque ripple in the SG are evaluated as a function of torque and speed for two different PWM strategies : Space Vector Modulation (SVM) and General Discontinuous PWM (GDPWM). Then a comparison is done to evaluate advantages and disadvantages of SVM and GDPWM.

II. INVERTER POWER LOSSES EVALUATION

The SG considered here is a wound rotor one represented in the stator reference frame (See Fig.1). Its neutral point is isolated. It is supplied by a battery which is here simply modeled by a DC voltage source. The SG is connected to the battery through a three-phased inverter. Both switches of a half bridge are switched alternately in order not to short-circuit the battery by respecting a dead time of one microsecond.

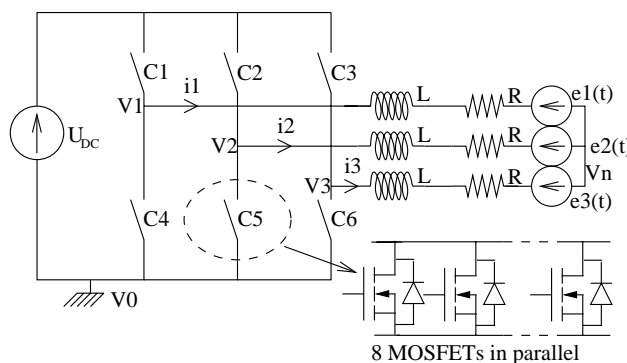


Fig. 1. Topology.

Practically, each of the six switches of the inverter is constituted by eight MOSFETs in parallel. Evaluation of power losses requires a precise model of the MOSFET in order to simulate real waveforms during switching phase and conduction phase. However it needs a very small step size which increases significantly the time of computation. To keep a reasonable step size, dissipated energy in a switch can be computed offline as a function of the type of command (turn on or turn off), the DC-link voltage U_{DC} and the chopped current I . As a result, evaluation of the losses in the inverter is possible while preserving a reasonable simulation time. The losses are divided into conduction losses and switching losses.

A. Conduction losses

When the switch is on, a MOSFET is considered as a simple resistance $R_{DS(on)}$ whatever the sense of the current. The value of this resistance increases with the junction temperature of the MOSFET [5]. Manufacturers give the evolution law of $R_{DS(on)}$ against junction temperature T_j . A second order interpolation function is used to approximate this law:

$$R_{DS(on)}(T_j) = C_0 + C_1 \cdot T_j + C_2 \cdot T_j^2 \quad (1)$$

The coefficients C_j are determined by a least-square method. The antiparallel diodes carry current only during the dead-time. The corresponding dissipated energy in the diode is also taken into account by considering the voltage drop when the current flows through it. The forward characteristic of the reverse diode is given by data sheets.

To evaluate the junction temperature, an equivalent scheme of the thermal circuit was established (See Fig.2).

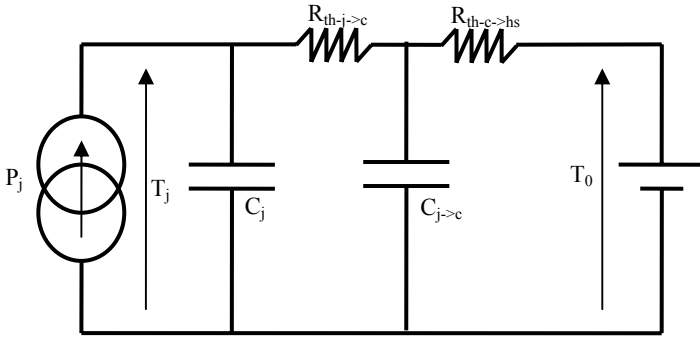


Fig. 2. Equivalent thermal circuit of the MOSFET.

The inverter is cooled by the cooling system of the vehicle characterized by the constant temperature T_0 . The MOSFETs are mounted on a water-cooled heat sink which is supposed to be perfect thus like a constant temperature source T_0 . The thermal resistance $R_{th-c \rightarrow hs}$ represents the support of the cases on the heat sink. $R_{th-j \rightarrow c}$ is the junction-to-case thermal resistance and C_j is the thermal capacity of the junction. The manufacturer data sheets give both. $C_{j \rightarrow c}$ represents the junction-to-case thermal capacity.

The dissipated power in the MOSFET is represented by a current source P_j . Equations of the circuit are solved by numerical computations and allow one to estimate evolution of T_j , $R_{DS(on)}$ and the voltage drop in the diode.

To precisely estimate temperature and losses vs. time, dissipated energy was dissociated between high side switch and low side switch which leads to six different thermal circuits (one per switch of the inverter).

This is very important because in some PWM strategies, the solicitation of the upper switch can be different from the solicitation of the lower one.

B. Switching losses

To interpolate switching losses, an half-bridge configuration is studied [6]. We consider the current $i_i(t)$ to be constant on a switching period $i_i(t)=I$. As far as there are two different types of switching command (rising edge and falling edge) and two different signs for the current I , there are four different analyses to perform. These analyses are summarized in the Table 1.

TABLE 1
FOUR DIFFERENT TYPES OF SWITCHES ON A HALF BRIDGE

		Switches type	
		Rising edge \nearrow	Falling edge \searrow
Current sign	$i > 0$	Highside MOSFETs turn-on	Highside MOSFETs turn-off
	$i < 0$	Lowside MOSFETs turn-off	Lowside MOSFETs turn-on

PSPICETM simulation results for the four cases of Table 1 are presented on Fig.3 for a DC-bus voltage of $U_{DC}=42$ V. The same simulations are repeated for different DC-bus voltages. By integrating these results, an approximation of the dissipated energy E_j in the MOSFET as a function of I and U_{DC} (See Fig.4) is established.

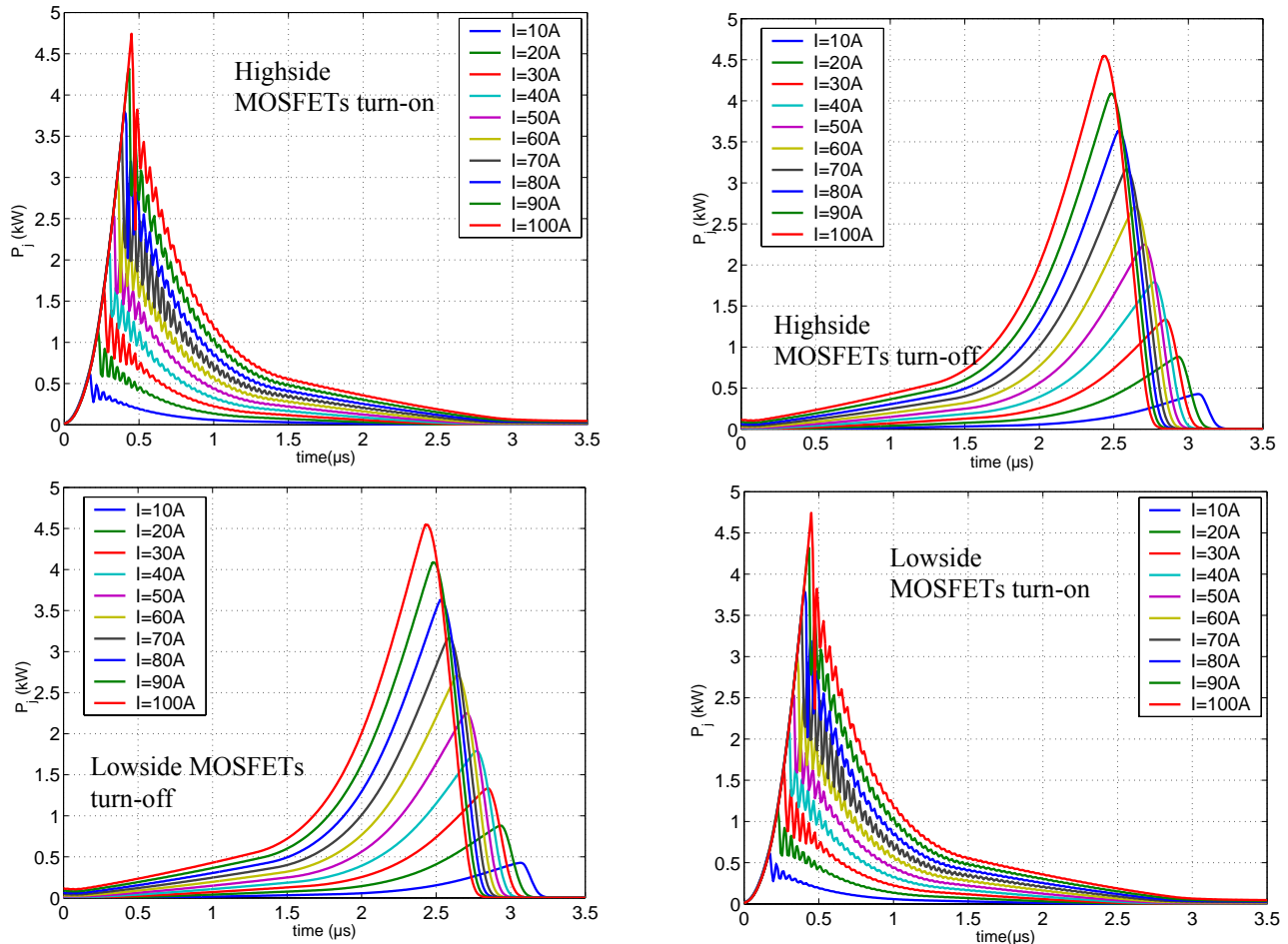


Fig. 3. Dissipated power for $U_{DC}=42$ V

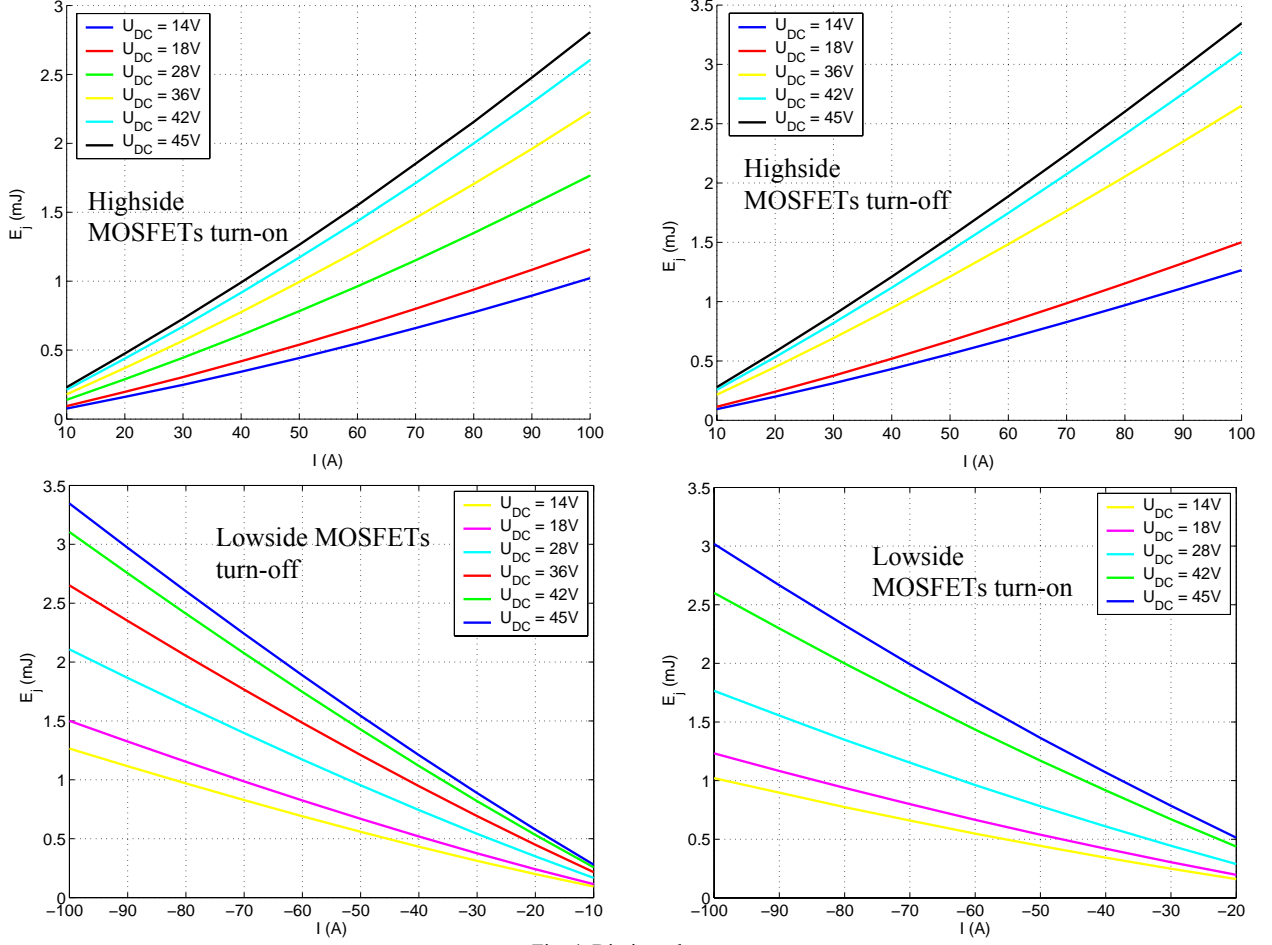


Fig. 4. Dissipated energy.

A simple analytical expression of the dissipated energy as a function of the DC-link voltage U_{DC} and I is:

$$E_j^*(U_{DC}, I) = (a \cdot U_{DC} + b) \cdot I^2 + (c \cdot U_{DC} + d) \cdot I \quad (2)$$

The coefficients (a,b,c,d) are determined by a least squares optimization routine:

$$\min_{(a,b,c,d)} \sum_{i=1}^n [E_j(i) - E_j^*(U_{DC}(i); I(i))]^2 \quad (3)$$

n is the number of simulation and $E_j(i)$ is the dissipated energy of simulation i . The numerical results are written in the Table 2. We can point out that the dissipated energy for a turn-on on the high-side switch and for a turn-on on the low side switch are identical. It is also the case for the turn-off. Consequently, the study can be limited to the dissipated energy of a single MOSFET in a simple chopper structure.

These results allow to know in advance the dissipated energy in a MOSFET at each switching command. As a result, a larger simulation step size can be adopted.

C. Numerical integration

These results are integrated into a large simulation of the SG application written in C/C++ language. They allow estimation of the dissipated energy for each of the three legs of the inverter (See Fig.5).

TABLE 2
INTERPOLATION COEFFICIENTS
Switches type

	Rising edge \mathcal{A}	Falling edge \mathcal{B}
$i > 0$	$a = 8.6987 \cdot 10^{-10}$ $b = 1.5738 \cdot 10^{-8}$ $c = 4.9811 \cdot 10^{-7}$ $d = -5.9438 \cdot 10^{-8}$	$a = 7.0193 \cdot 10^{-10}$ $b = 2.3197 \cdot 10^{-8}$ $c = 5.5394 \cdot 10^{-7}$ $d = 2.8620 \cdot 10^{-6}$
Current sign $i < 0$	$a = 7.0193 \cdot 10^{-10}$ $b = 2.3197 \cdot 10^{-8}$ $c = 5.5394 \cdot 10^{-7}$ $d = 2.8620 \cdot 10^{-6}$	$a = 8.6987 \cdot 10^{-10}$ $b = 1.5738 \cdot 10^{-8}$ $c = 4.9811 \cdot 10^{-7}$ $d = -5.9438 \cdot 10^{-8}$

Interpolation of both switching losses and conduction losses permits to estimate efficiency of the inverter for different operating points of the SG as a function of the PWM strategy.

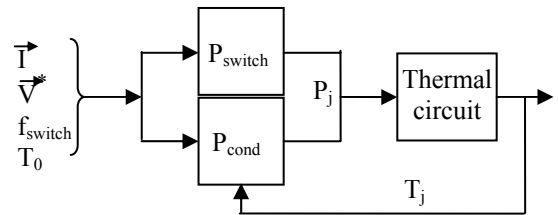


Fig. 5. Simulation synoptic

III SVM AND GDPWM STRATEGIES

Reduction of losses in the inverter is a way to achieve reduction of the size of the converter. Two possibilities can be considered:

- reducing conduction losses by improving the thermal circuit (with a better application of the cases on the heat sink) or by changing MOSFET technology with a lower $R_{DS(ON)}$. It requires physical modification of the converter.
- reducing switching losses by decreasing the switching frequency without modifying quality of phase currents. It can be done by using Discontinuous PWM strategies (DPWM) [7].

A. Torque control

The torque control of the SG is obtained by a regulation in d-q axis (See Fig.6). The PWM control determines the three switching functions of the inverter legs. The electrical machine is a belt-driven one with a 3:1 ratio. Consequently, high speed can be reached (18000 RPM).

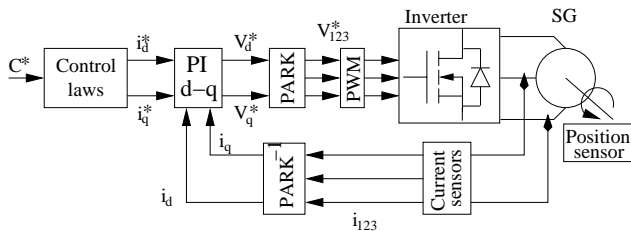


Fig. 6. Regulation in d-q axis

The torque-speed plan of the specifications is plotted on Fig.7. It is characterized by:

- high torque at low speed in starter mode in order to start the thermal engine
- positive torque at medium and high speed in boost mode in order to increase the total mechanical power available
- negative torque at medium and high speed in alternator mode in order to generate electrical power to supply electrical equipments

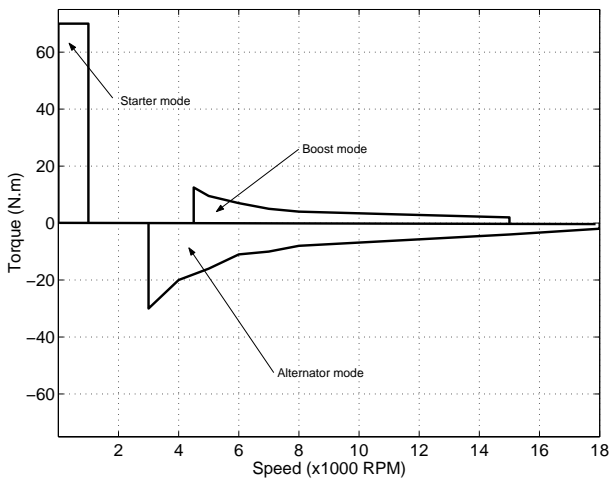


Fig. 7. Useful torque-speed plan of a separated SG

The torque-speed plan is generalized by a symmetrical one in the next paragraphs.

B. Space vector modulation

We first consider a SVM strategy to drive the inverter. SVM is a very common strategy to control a three-phased inverter [8][9]. There are several techniques which differ in the position of the PWM pulses in the switching period. We here consider the classical one with centered pulses [10] (See Fig.8). It is particularly suited to implementation in a DSP as far as it is a direct digitalized technique. We can evaluate power losses of the converter and torque ripple of the SG under SVM for each operating point of the torque-speed plan in steady-state operation.

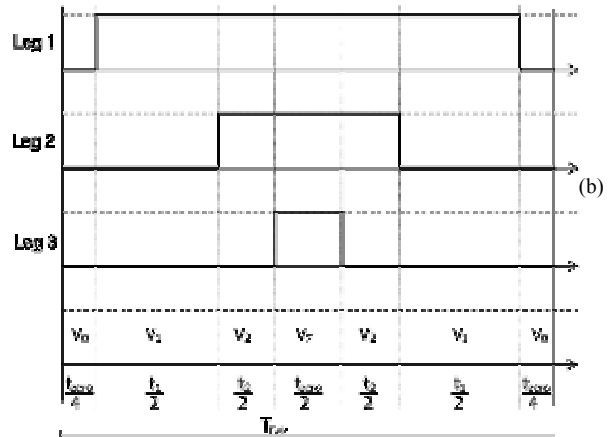
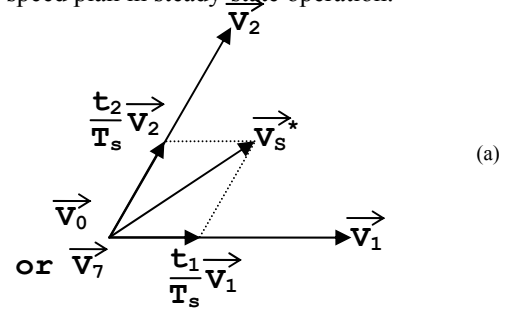


Fig. 8. (a) Reference voltage vector decomposition (b) Corresponding centered pulses SVM

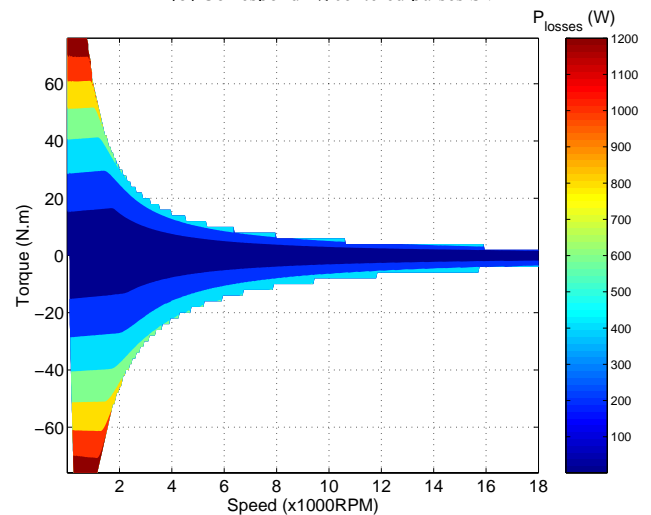


Fig. 9 Power losses in the inverter under SVM strategy

Power losses increase in the low speed – high torque region because high current occurs (up to 500 A). One can see that power losses are directly proportional to the magnitude of the current vector. The converter efficiency is always better than 90% in the full operating area.

In order to verify the quality of the PWM strategy, the torque ripple of the SG is calculated. We consider the rms value defined by:

$$\Delta C = \sqrt{\frac{1}{T} \int_{t_0}^{t_0+T} (C(t) - \langle C \rangle)^2 dt} \quad (4)$$

Results are presented on Fig.10. We can achieve a very precise control of the SG even at high speed. The level of the torque ripple remains relatively low. The harmonic distortion of the phase voltage induced by the PWM strategy is responsible of the torque ripple. This harmonic distortion is minimum when the reference voltage vector describes the largest inscribed circle in the hexagon formed by the available voltage vectors. As a result, the low level of the torque ripple on the operating area can be explained by the fact that we often use the maximum of voltage available in PWM mode.

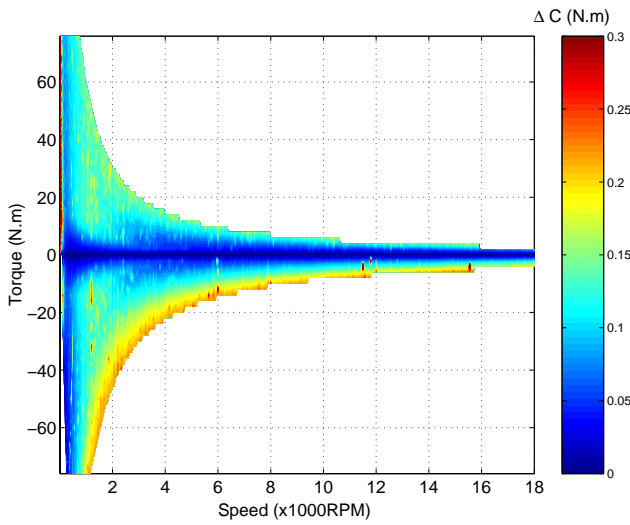


Fig. 10. Torque ripple of the SG under SVM strategy

C. General Discontinuous PWM

The basic idea of DPWM (Discontinuous PWM) is to stop switching a half bridge for one third of the period [11]. It means that there is always one half bridge that does not switch. In general, the third of the period is divided in two sixth of the period. During the first one, the half bridge is maintained at the upper level whereas during the other, it is maintained at the lower level (See Fig.11).

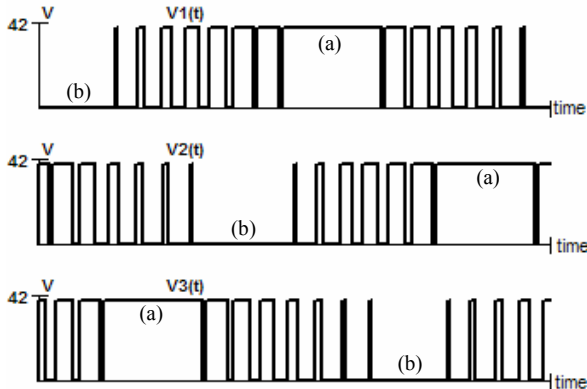


Fig. 11. example of DPWM pulses
(a) Half bridge maintained at the upper level
(b) Half bridge maintained at the lower level

These strategies are also known as two-phase modulation. DPWM techniques vary with the position of the stop switching times in the period.

The maximum effectiveness of DPWM appears when the half bridge stops switching exactly when the corresponding current is the highest. The idea of GDPWM (General Discontinuous PWM) is to choose the ideal moment as a function of the phase shift between current and voltage. Reference [7] gives an exhaustive explanation of GDPWM. As far as two other half bridges switch at the same frequency as the SVM, the average switching frequency of GDPWM is $\frac{2}{3} f_{SVM}$.

To compare with SVM, we have done the same simulation in steady-state operation for each operating point of the torque-speed plan. Results are given on Fig.12 and Fig.13.

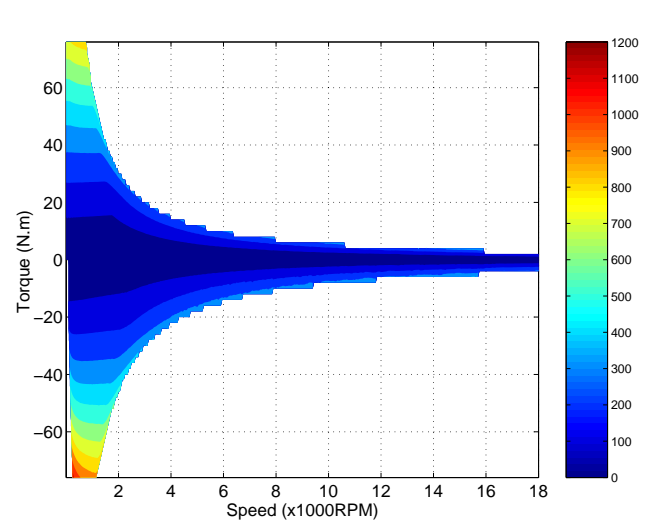


Fig. 12. Power losses in the inverter under GDPWM strategy

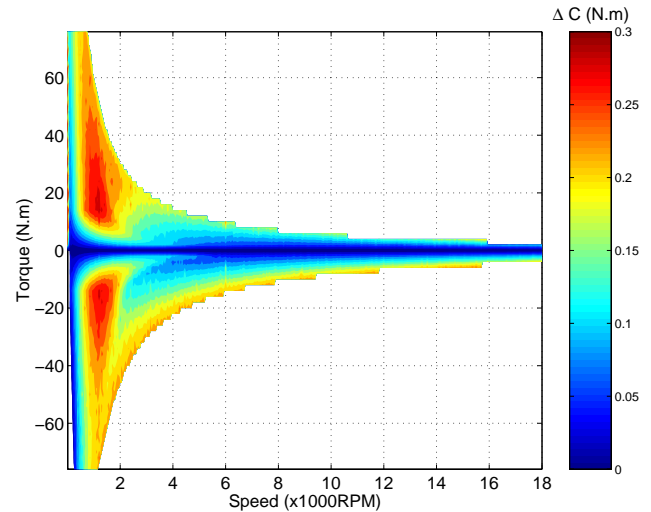


Fig. 13. Torque ripple of the SG under GDPWM strategy

As we use the same scale for SVM and GDPWM, it is obvious that power losses in the inverter decrease under GDPWM strategy whereas the torque ripple of the SG increases in some areas of the torque-speed plan.

IV. COMPARISON

A. Power losses in the inverter and torque ripple

As far as the average switching frequency of GDPWM is $\frac{2}{3} f_{SVM}$, switching losses are decreased between 25% and 50% compared to those induced by SVM strategy. The total power losses are significantly reduced in the whole operating area (See Fig. 14). The "Gain" is defined by

$$Gain = \frac{X_{GDPWM} - X_{SVM}}{X_{SVM}} \cdot 100\% \text{ where } X \text{ is the power losses (Resp. Torque ripple) on Fig. 14 (Resp. Fig. 15).}$$

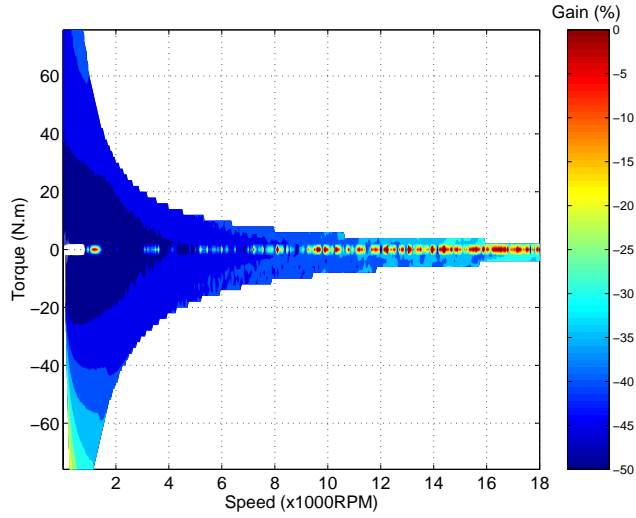


Fig. 14 Gain in terms of power losses

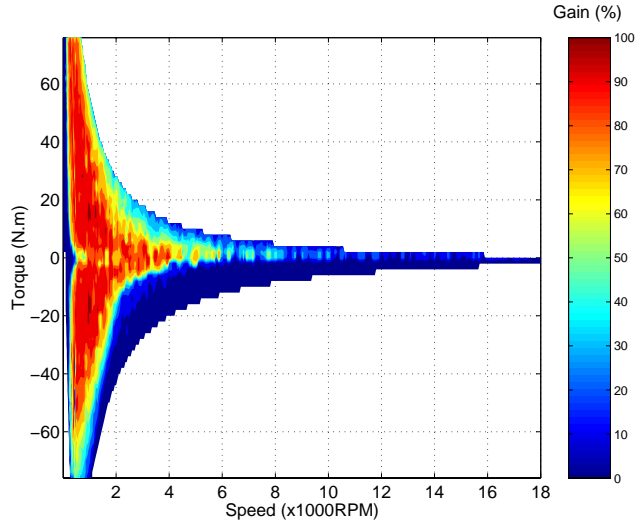


Fig. 15 Gain in terms of torque ripple

The torque ripple can be multiplied by a factor two in some areas. Both results show that a compromise must be done to choose between GDPWM and SVM.

B. Focus on specific operating points

To illustrate this compromise, some simulations were done for three specific operating points : a starter point, a boost point and an alternator point. For different switching frequencies, we plot the power losses of the inverter versus the torque ripple for SVM and GDPWM.

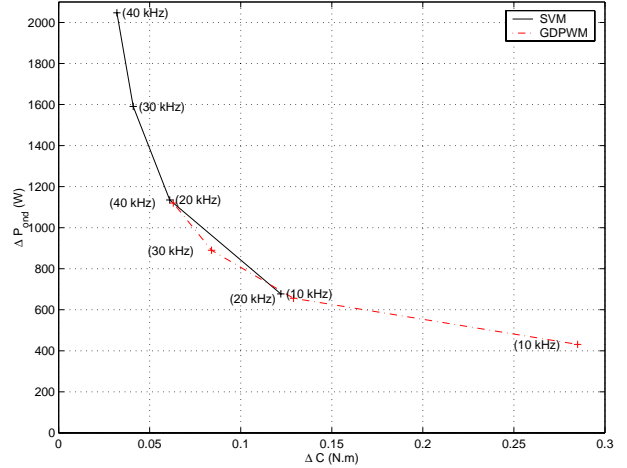


Fig. 16 Power losses versus torque ripple for a starter point

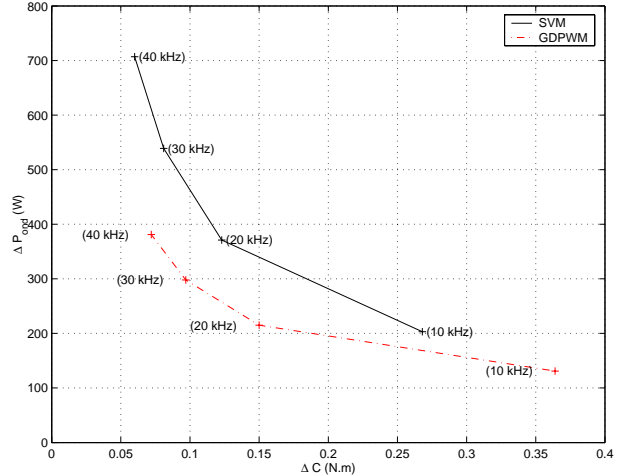


Fig. 17 Power losses versus torque ripple for a boost point

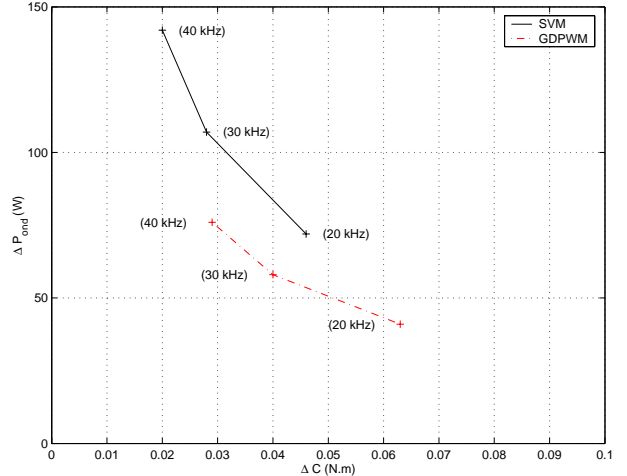


Fig. 18 Power losses versus torque ripple for an alternator point

One can see that the compromise is evident whatever the operating point. In fact for a given switching frequency, SVM is characterized by higher power losses than GDPWM but lower torque ripple.

It is also important to point out that for the same average switching frequency (for example, GDPWM at 30 kHz on Fig. 16~18 has an average frequency of 20 kHz), the GDPWM presents lower torque ripple and lower power losses than SVM for the alternator point and boost point whereas for the starter point. However, it requires MOSFETs able to switch at higher frequency for two third of an electrical period.

C. Integration under SG application constraints

Phase voltage distortion under PWM strategy is responsible of torque ripple. In function of the magnitude of the reference voltage vector \vec{V}^* , we define the Weighted Total Harmonic Distortion (WTHD) by :

$$WTHD = \frac{\sqrt{\sum_{n=2}^{\infty} \frac{V_n^2}{n^2}}}{V_1} \quad (5)$$

It represents the harmonic distortion balanced by a coefficient $1/n$ for the n -order harmonic.

We also define the modulation index M_i which represents the magnitude of the reference voltage vector compared to the full wave fundamental magnitude :

$$M_i = \frac{\|\vec{V}^*\|}{\frac{2}{\pi} U_{DC}} \quad (6)$$

The WTHD is plotted for SVM and GDPWM strategy (See Fig.19).

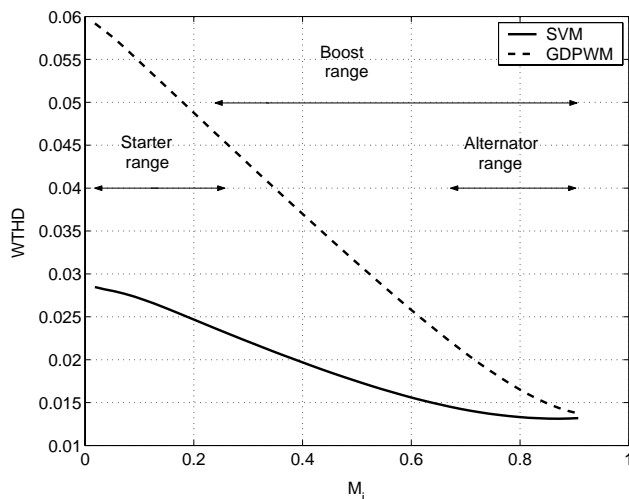


Fig. 19 WTHD of SVM and GDPWM

In alternator mode, the maximum of voltage is often used. The difference in terms of WTHD is relatively low and GDPWM can be used in this mode to obtain inverter power losses gain. Moreover, the alternator mode is frequent and GDPWM can result in an increase of reliability.

The starter mode lasts a short time but high currents occur and the inverter is highly constrained. In the corresponding range of voltage, the WTHD is high and consequently the torque ripple can increase. The choice between the two strategies must integrate:

- the degradation of the start quality because of increase of the torque ripple
- the compromise between inverter stress and start quality.

V. CONCLUSION

As far as GDPWM only needs software modification and can be implemented in a DSP, it does not require any geometrical modifications.

In regard of the high stresses of the inverter of a SG application, GDPWM can be a good way to achieve reduction of power losses in the inverter.

However, it implies increase in torque ripple. Only experiments can determine if it can modify the vehicle comfort of control.

Eventually, in function of the thermal stress of the inverter and/or the style of control of the driver, a supervisor can switch between SVM and GDPWM. It can also be implemented in a dedicated chip (FPGA or ASIC).

REFERENCES

- [1] J.G. Kassakian "The role of power electronics in future 42 V automotive electrical systems" EPE Journal, vol.13(N°4), November 2003.
- [2] L. Chédot and G. Friedrich, "Optimal control of interior permanent magnet synchronous integrated starter-generator" EPE 2003, Toulouse, September 2003.
- [3] C. Plasse, A. Akemakou, P. Armiroli, and D. Sebillé "L'alternodémarrreur, du stop&go au groupe motopropulseur mild hybride" Prop'Elec, Aix-en-Provence, March 2003.
- [4] A.F. Petrie and C. Hymowitz "Spice model accurately simulates IGBT parameters" Power-conversion & Intelligent Motion, vol.22(N°1), January 1996.
- [5] C. Buttay "Estimateur de température et de courant dans un pont en H à base de MOSFET" JCGE'03, Saint-Nazaire, June 2003.
- [6] M. Bland, P. Wheeler, and J. Clare. "Comparison of losses in voltage source inverters and direct ac-ac converters" EPE Journal, vol.13(N°1), February 2003.
- [7] A.M. Hava, R.J. Kerkman, and T.A. Lipo "A high performance generalized discontinuous pwm algorithm" IEEE Transactions on Industry Applications, vol.34(N°5), September/October 1998.
- [8] H.W. Van Der Broeck, H.Ch Skudelny, and A. Nabae "Analysis and realization of a pulse width modulator based on voltage space vectors" IEEE/IAS Annual Meeting Conference Record, vol.29,pp.412-17, 1988.
- [9] S. Ogasawara, H. Akagi, and G. Stanke "A novel pwm scheme of voltage source inverters based on space vector theory" Archiv für Elektrotechnik, vol.74,pp.33-41, 1990.
- [10] F. Jenni and D. Wueest "The optimization parameters of space vector modulation" Fifth European Conference on Power Electronics and Applications, IEE - London - UK, 1993.
- [11] J.P. Cambronne, Ph. Le Moigne, and J.P. Hautier "Synthèse de la commande de l'onduleur de tension" Journal de Physique III, 1996.